RESEARCH LETTER

Key Points:
- Aerosols dominated the distributions of past large-scale precipitation change
- Aerosol forcing caused surface temperature gradient is responsible for such change

Supporting Information:
- Text S1, Table S1, and Figures S1–S4

Correspondence to:
C. Wang,
wangc@mit.edu

Anthropogenic aerosols and the distribution of past large-scale precipitation change

Chien Wang[1]

[1]Center for Global Change Science, Massachusetts Institute of Technology, Cambridge, Massachusetts, USA

Abstract The climate response of precipitation to the effects of anthropogenic aerosols is a critical while not yet fully understood aspect in climate science. Results of selected models that participated the Coupled Model Intercomparison Project Phase 5 and the data from the Twentieth Century Reanalysis Project suggest that, throughout the tropics and also in the extratropical Northern Hemisphere, aerosols have largely dominated the distribution of precipitation changes in reference to the preindustrial era in the second half of the last century. Aerosol-induced cooling has offset some of the warming caused by the greenhouse gases from the tropics to the Arctic and thus formed the gradients of surface temperature anomaly that enable the revealed precipitation change patterns to occur. Improved representation of aerosol-cloud interaction has been demonstrated as the key factor for models to reproduce consistent distributions of past precipitation change with the reanalysis data.

1. Introduction

The quantity of global total precipitation change is shown to respond robustly to the global mean surface temperature change, whereas the spatial distribution of such change carries significant regional characteristics and can be influenced by many factors including atmospheric circulation change [e.g., *Mitchell et al.*, 1987; *Allen and Ingram*, 2002; *Held and Soden*, 2006]. It has been indicated that persistent anthropogenic aerosol forcings alone could alter atmospheric circulation and hence the large-scale precipitation distribution. Added by the asymmetrical distribution of aerosols that weighs more substantially over the Northern than Southern Hemisphere, these effects would lead to a shift of tropical precipitation toward the relatively warming hemisphere, i.e., the Northern Hemisphere if forced by absorbing aerosols [*Wang*, 2004], or the Southern Hemisphere if forced by scattering aerosols or the clouds with enhanced reflectance owing to anthropogenic aerosols (i.e., the indirect effects of aerosols) [*Ramaswamy and Chen*, 1997; *Rotstayn and Lohmann*, 2002]. With assistance of modeling results, there have also been attempts to attribute certain observed precipitation changes in the past to the influence of anthropogenic aerosols [e.g., *Zhang et al.*, 2007; *Hwang et al.*, 2013; *Wu et al.*, 2013; *Polson et al.*, 2014; *Osborne and Lambert*, 2014] besides natural variability [e.g., *Salzmann and Cherian*, 2015]. However, insufficient temporal coverage of historic precipitation records has made such detection and attribution efforts rely heavily on modeled aerosol forcing and response patterns. Using results produced by the models with overly simplified representation of aerosol-cloud interaction, as demonstrated in this study, could prevent one from distinguishing the response to anthropogenic aerosols from that of greenhouse gases.

Questions, hence, remain that whether the precipitation responses to aerosol effects derived from cases with aerosol forcing alone would still be significant when greenhouse gas forcings coexist, especially when feedbacks to aerosol forcings in different scales were involved [e.g., *Lohmann et al.*, 2010; *Myhre et al.*, 2013; *Wu et al.*, 2013], and whether the transient historical simulations using models with improved representation of aerosol-cloud interaction could help us to better identify the aerosol effects from observed precipitation changes.

The recent Coupled Model Intercomparison Project Phase 5 (CMIP5) [*Taylor et al.*, 2012] has included a sizable group of models with features of interactive aerosol and prognostic cloud microphysics as well as aerosol-cloud microphysics connection to perform different sets of climate simulations. This has provided us with the opportunity, for the first time, to examine the climate responses to anthropogenic aerosols with prognostic aerosol-cloud interaction, using results from long transient simulations projected by an ensemble of models instead of a single model.

2. Models, Data, and Results

In this study, 10 models that participated the CMIP5 and included interactive aerosol and prognostic cloud microphysics were selected to analyze the impacts of anthropogenic aerosols on global precipitation changes since preindustrial time. Here the interactive (or online) aerosol feature is represented by the dynamically predicted aerosol distribution in the atmosphere based on emissions, transport, and scavenging, calculated using predicted wind and rainfall, and by the model radiation calculations using dynamically predicted aerosol distributions. These models will be referred to as group 1 (G1) models hereafter (see supporting information).

Specifically, the results of each model from three transient simulations integrated from 1850 to 2005 were used in analyses. These include the following: (a) "Historical" (the simulation including all transient anthropogenic and natural forcings), (b) "HistoricalGHG" (same as Historical but only including forcings of long-lived greenhouse gases), and (c) "HistoricalNAT" (excluding all anthropogenic forcings while including transient "natural forcings" such as volcanic aerosols and the Earth's orbital change). The transient climate changes of variables including surface air temperature and precipitation were represented by the anomalies of these variables in reference to their last 100 year means in the corresponding long preindustrial control simulations (piControl) and used in analyses. Since the number of sensitivity simulations that included only anthropogenic aerosol effects was rather small, the transient climate response to anthropogenic aerosols, along with ozone and the land use change for each selected model, was actually derived by subtracting the responses obtained in HistoricalGHG and HistoricalNAT from that in Historical simulations (see supporting information). The corresponding results are referred to as HistoricalNonGHG hereafter. This is similar to the method used in several previous CMIP5-based analyses [*Forster et al.*, 2013; *Shindell*, 2014], assuming that the above responses are linearly additive [*Ramaswamy and Chen*, 1997].

Notably, among the nongreenhouse gas anthropogenic forcings, that of aerosols is nearly 3–4 times larger in absolute quantity than either ozone or the land use change and thus is the dominant component among these forcings [*Shindell*, 2014]. In addition, among aerosol effects, the indirect effect of aerosols, i.e., the radiative effect resulting from the modification of cloud reflectance or lifetime by aerosols through the aerosol-cloud microphysical connection, is estimated to be substantially larger than the direct aerosol effect, i.e., the radiative effect resulting from the direct absorption or scattering of sunlight by aerosols [*Myhre et al.*, 2013; *Shindell*, 2014].

Recent analyses have suggested that physically based parameterizations of aerosols and aerosol-cloud interaction could be a critical feature for models to reproduce observed past temperature and precipitation trend [*Ekman*, 2014; *Wilcox et al.*, 2013]. In order to examine the importance of modeled features of aerosols and clouds regarding precipitation responses, seven additional models were added to the analyses. These models either prescribed direct aerosol radiative effect or included both direct and indirect effect, but the latter was formulated in a parameterization without prognostic cloud microphysical features. These models will be referred to as group 2 (G2) models hereafter (see supporting information). Notably, the majority if not all of the models that participated previous CMIP3 program are the same type as G2 models.

The information of aerosol direct and indirect effects used in the transient simulations by the selected CMIP5 models is incomplete. A thorough comparison of these effects between G1 and G2 models is thus difficult. Still, based on *Shindell* [2014], it can be found that the direct radiative forcing at year 2000 in reference to 1850 of the only G2 model listed there is about 0.16 to 0.73 W/m^2 lower than those of other seven listed models that are categorized as G1 models in this study (−0.71 versus −0.87 to −1.44 W/m^2). Deriving the exact difference in indirect effects is even more difficult. However, it can be estimated by using indicators for indirect effects such as the solar band cloud forcing (all-sky minus clear-sky outgoing radiative fluxes at the top of the atmosphere). The difference in global mean solar band cloud forcing between the G1 and G2 model ensembles is found to be 0.32 W/m^2 in the Historical simulations, or a substantial value.

Reliable global observations of precipitation covering both land and ocean are still too short to evaluate these historical model simulations throughout their entire integration periods. In this study, the Twentieth Century Reanalysis Data Version 2C [*Compo et al.*, 2011] was used as the observational base for both surface air temperature and precipitation. The 30 year means from 1946 to 1975 were used as the base values to derive the anomalies of precipitation and surface air temperature in the analysis period of 1976 to 2005. The same analysis period is also selected for the modeled results as it represents the last 30 years of the 1850–2005 transient simulations and as the satellite retrievals become available in recent decades.

It is found that the ensemble precipitation change produced by G1 models in the Historical simulation shares many similar patterns with HistoricalNonGHG in particular over the tropics. When averaged over a 30 year period of 1976–2005, a precipitation reduction in the northern hemispheric branch of the Intertropical Convergence Zone (ITCZ) can been seen in both ensembles, which extends almost continuously along the zonal direction from the tropical Pacific, Atlantic, and Indian Oceans, to the Maritime Continent (Figures 1a and 1c). Mirroring this reduction is an enhancement of precipitation along the southern hemispheric tropics, with a less extent in continuity and a peak over the central and eastern Pacific. Another similarity between these two sets of simulations is a precipitation reduction extending from the Maritime Continent northward to East China, entering the northern hemispheric midlatitude. The same southward shift of precipitation over the ITCZ can be also seen in the reanalysis data particularly over the tropical Pacific, Atlantic, and Indian Oceans (Figures 1g and 1h). The patterns of the reanalysis result over the Maritime Continent, however, can be quite different than the modeled features, depending on the choice of reference for deriving the anomalies; this is also true for the precipitation reduction along East China. On the other hand, the ensemble precipitation change derived from HistoricalGHG simulation exhibits a zonally distributed enhancement within the tropics, centered at the equator (Figure 1b).

Beyond the tropics, the G1 ensembles of Historical and HistoricalNonGHG along with reanalysis data all display more precipitation reduction than enhancement in the midlatitude of both hemispheres. In the high latitudes of both hemispheres, the G1 HistoricalGHG ensemble derives a rather strong precipitation enhancement while the G1 Historical ensemble and the reanalysis data only show a moderate increase, whereas the G1 HistoricalNonGHG ensemble displays a reduction. The pattern correlation between the G1 Historical and HistoricalNonGHG ensemble is 0.58, whereas the pattern correlation between the G1 Historical and HistoricalGHG ensemble is only 0.25. In contrast, the G2 Historical ensemble of precipitation change shows many similarities with the HistoricalGHG (pattern correlation = 0.39) rather than HistoricalNonGHG ensemble (pattern correlation = 0.28), over both the tropical and extratropical regions (Figures 1d–1f). Note that all these model ensemble distributions do not change evidently when the reference for deriving the anomalies is switched from the last 100 year mean of the piControl to the 1946–1975 mean; only the quantities of precipitation change become smaller (Figure S1 in the supporting information).

The similarities along with differences among various model ensembles and reanalysis data can be better explained through the variability analysis, e.g., the method of empirical orthogonal function (EOF). From 1976 to 2005, the major variability patterns, or the first two EOFs of the zonal precipitation changes derived from the G1 Historical and HistoricalNonGHG ensembles as well as the reanalysis data, are almost identical (Figure 2, top). All have a pair of variance peaks with opposite signs separated almost perfectly by the equator as the first EOF, reflecting the precipitation center shift in the ITCZ. Their second EOF consists of a variance peak centered at the equator surrounded by a pair of opposite variance peaks, which is almost identical in pattern to the first EOF of G1 HistoricalGHG. In comparison, the second EOFs of the G2 Historical and HistoricalNonGHG ensembles share the same pattern with the first EOFs of the G1 Historical and HistoricalNonGHG ensembles as well as reanalysis data, whereas the first EOFs of these G2 ensembles have the same pattern of the second EOFs of the G1 Historical as well as HistoricalNonGHG ensembles and the reanalysis data or the first EOF of the G1 HistoricalGHG ensemble, implying that greenhouse gases rather than aerosols have mainly influenced the major tropical precipitation changes in G2 models. When reconstructed using the first three EOFs, the 1976–2005 mean of zonal precipitation changes of the G1 Historical ensemble follows the reanalysis data very well across almost all the latitudes, except for having a smaller amplitude, whereas the G2 Historical ensemble has a clearly different pattern in comparison, especially over the tropics (with a peak enhancement across the equator) as well as most extratropical latitudes in the Northern Hemisphere (Figure 2, bottom left). Reconstructed precipitation responses of the G1 and G2 HistoricalGHG ensembles are largely identical, whereas those of HistoricalNonGHG ensembles are very different (Figure 2, bottom right). This clearly suggests that the major reason behind the differences between the G1 and G2 Historical ensembles is their different aerosol forcing strengths.

The zonal mean patterns of precipitation changes derived in the G1 Historical and HistoricalNonGHG ensembles have largely been persistent throughout the second half of the twentieth century and become quantitatively more substantial after the 1970s until the early 1990s (Figure S2). The persistent shift of precipitation in the ITCZ also exists in the reanalysis data, whereas the latter display larger amplitudes of interannual variation than the modeled results. Particularly, over the tropics all these three distributions differ distinctively from the results of the G2 Historical ensembles.
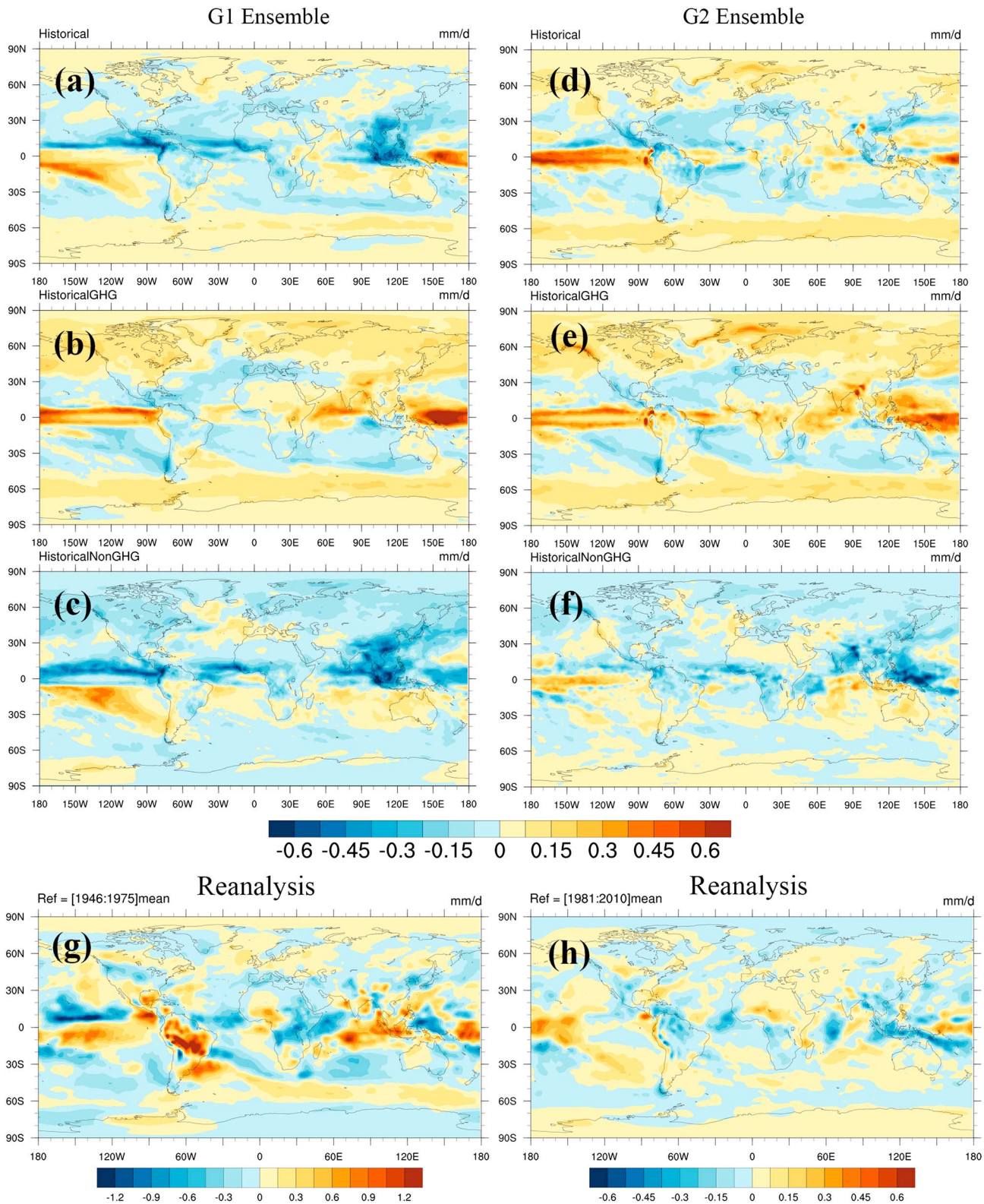
Figure 1. Ensemble precipitation changes of G1 models in (a) Historical, (b) HistoricalGHG, and (c) HistoricalNonGHG and G2 models in (d) Historical, (e) HistoricalGHG, and (f) HistoricalNonGHG. All data are 1976–2005 annual means in reference to the last 100 year mean of the corresponding preindustrial control simulation. Also shown are 1976–2005 annual mean precipitation changes derived from the reanalysis data using, as reference, (g) the 1946–1975 mean (note that a different color scale is used) or (h) the 1981–2010 mean.
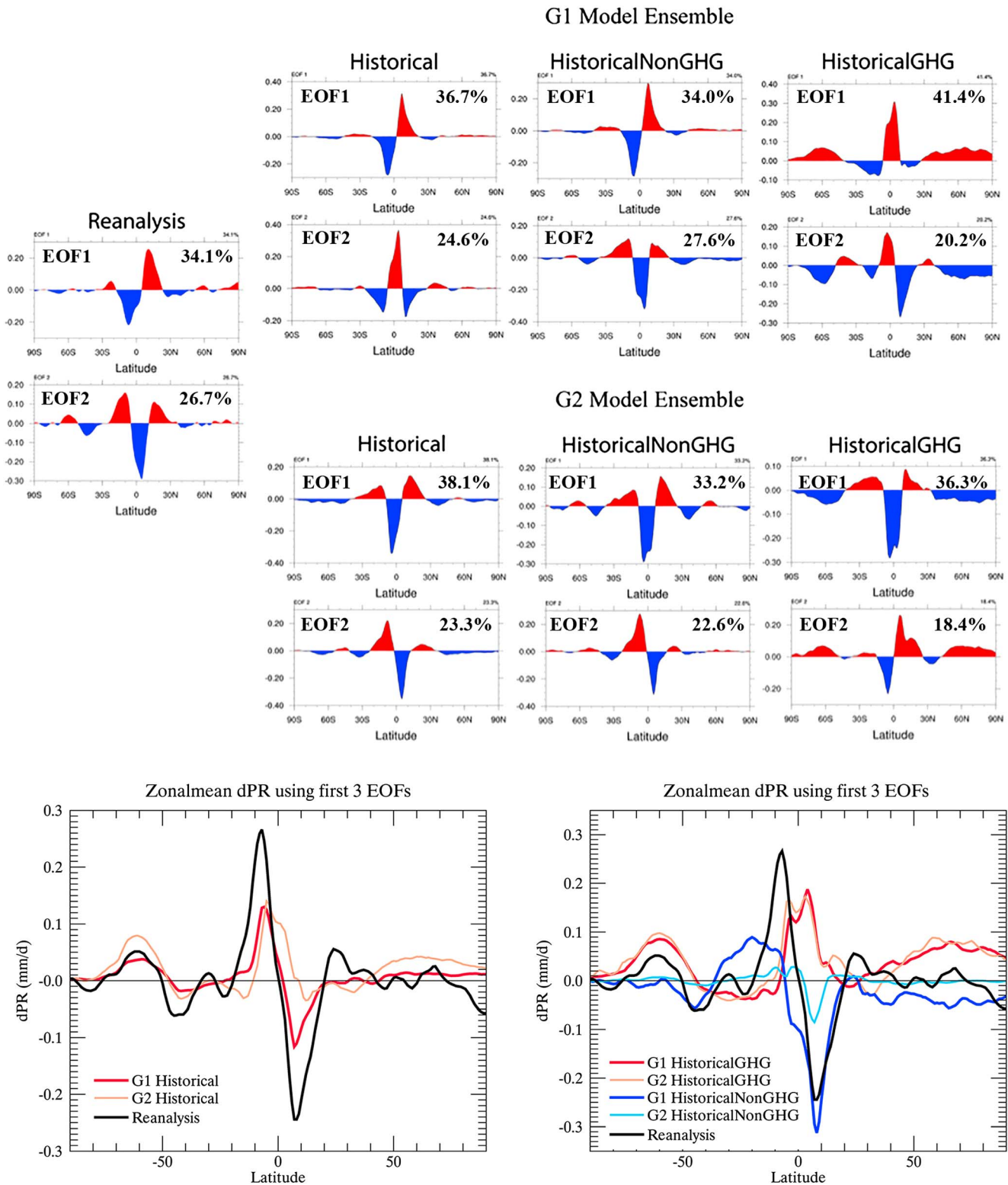
Figure 2. (top) The first two EOFs derived from the reanalysis data as well as various model ensembles. (bottom, left) Reconstructed precipitation anomalies using the first three EOFs of the G1 and G2 Historical ensembles and the reanalysis data. (bottom, right) Reconstructed precipitation anomalies using the first three EOFs of the G1 and G2 HistoricalNonGHG as well as HistoricalGHG ensembles. All modeled quantities are averaged over 1976 to 2005 in reference to the last 100 year mean of the corresponding control simulations. The reanalysis result is also the 1976 to 2005 mean but in reference to the 1946 to 1975 average. First three EOFs represent 68.5% of precipitation variance in reanalysis data; 70.0%, 70.5%, and 76.3% in G1 Historical, HistoricalNonGHG, and HistoricalGHG ensemble, respectively; and 72.4%, 64.8%, and 68.4% in G2 Historical, HistoricalNonGHG, and HistoricalGHG ensemble, respectively.
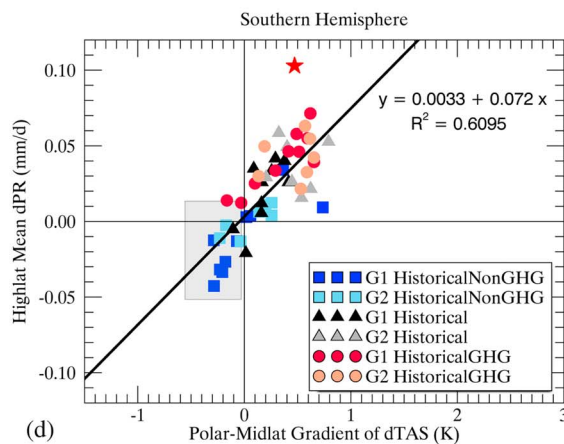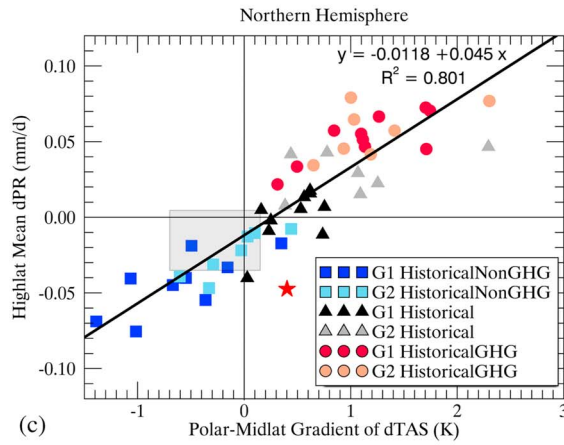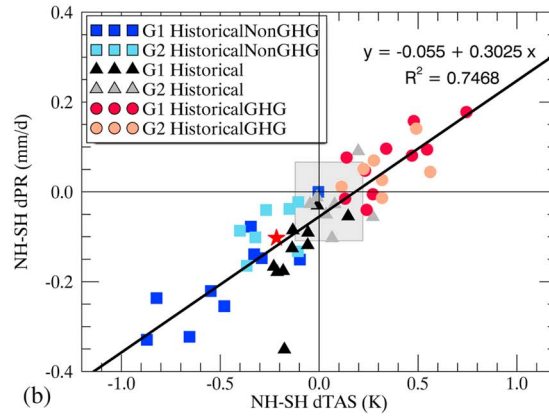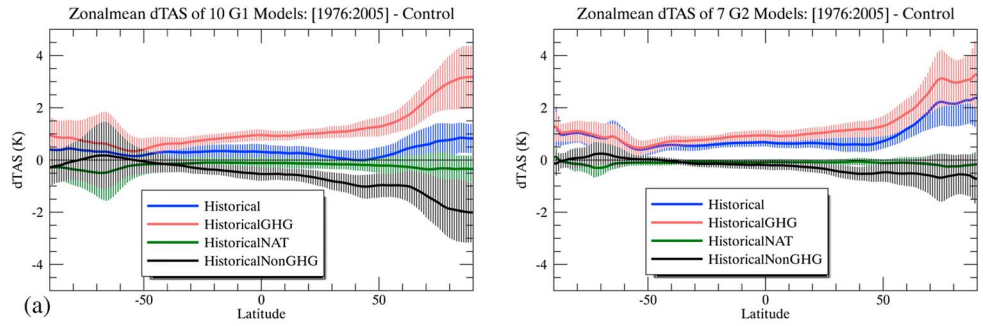
Figure 3

Anthropogenic aerosols are distributed more intensely over the Northern than Southern Hemisphere. The asymmetric cooling at the Earth's surface brought by aerosol forcings has induced a hemispheric gradient of surface temperature anomaly despite a significant and cross-latitude warming by greenhouse gases (Figures 3a and S3). Such a gradient appears to be the reason behind the revealed pattern of tropical precipitation change in the G1 ensemble and reanalysis data, consistent also with the results of previous idealized climate simulations driven by prescribed hemispheric cooling or heating [*Chiang and Bitz*, 2005; *Broccoli et al.*, 2006; *Kang et al.*, 2008]. Note that in comparison, surface temperature and its trends in recent decades across the Northern Hemisphere derived from the G1 ensemble are lower in value and more consistent with the observations than those from the G2 ensemble (Table S1).

Discussions on the shift of precipitation over the ITCZ in responding to asymmetric forcing have increased recently. Besides the correlation of such a shift to the hemispheric thermal gradient [*Chiang and Friedman*, 2012], a diagnostic using cross-equatorial flux of moist static energy to identify the location and thus estimate the shift of the ITCZ has also been suggested [*Hwang et al.*, 2013; *Bischoff and Schneider*, 2014]. However, many factors besides anthropogenic aerosols could affect the calculation of cross-equator heat transport, e.g., El Niño–Southern Oscillation (ENSO) that would create a response similar to that by aerosols [e.g., *Wang*, 2007; *Schneider et al.*, 2014]. This would make the attempt of attributing the observed ITCZ shift to the aerosol effects rather difficult, added by the lack of prognostic aerosol and cloud features in previous generation of models. Since the aerosol-induced atmospheric energy deficit can be directly related to the nonuniform surface temperature change, therefore, here the hemispheric gradient of surface temperature change has been correlated directly with the tropical precipitation change pattern, and such a correlation is found to be robust for all selected G1 and G2 models in various sets of simulations as well as for the reanalysis data (Figure 3b), demonstrating that the hemispheric thermal gradient is a good driver for the change of tropical precipitation distributions. Again, G1 models produced stronger hemispheric thermal gradients as well as southward shifts of tropical precipitation than G2 models, making the corresponding Historical results clearly differ from HistoricalNAT (7 out of 10 models) and also consistent with the reanalysis data. In comparison, most (5 out of 7 models) G2 models displayed an insignificant response in the Historical simulations comparing to the results of HistoricalNAT.

Beyond the tropics, the impacts of aerosol effects on precipitation are also evident in many zones. In the polar regions, greenhouse gas forcing has introduced a greater warming than in the midlatitude, and thus a sharp pole-midlatitude gradient of surface temperature anomaly (not necessarily the gradient of surface temperature itself). Such a gradient forced by greenhouse gases would reduce the negative pole to midlatitude temperature gradient and make the polar front and associated precipitation move poleward. This is actually what has been reflected in the results of the Southern Hemisphere, where both the G1 and G2 model ensembles have produced a peak of precipitation change mostly south of 60°S (Figure 3d). Note that all models have underestimated this precipitation enhancement compared to the reanalysis data. On the other hand, in the Northern Hemisphere, aerosol effects exerted a strong cooling over the high latitudes and polar region that nearly offset the warming caused by greenhouse gases. The middle- and high-latitudinal surface temperature amplification is more realistic in the G1 ensemble than in the G2 ensemble when comparing to the observations [*Ekman*, 2014] (see Table S1). As a result, high-latitude precipitation changes derived from both the G1 ensemble and the reanalysis data appear to have almost no trend at all (Figure 3c). This has answered the question about the missing midlatitude precipitation trend in the Northern Hemisphere raised in a previous analysis based on observations [*Osborne and Lambert*, 2014] and clearly demonstrated the critical role of aerosol effects in determining the large-scale distribution of past precipitation change in regions even beyond the tropics.

Figure 3. (a) The ensembles of zonal mean surface temperature changes of (left) 10 group 1 (G1) models and (right) 7 group 2 (G2) models in Historical, HistoricalGHG, HistoricalNAT, and HistoricalNonGHG, respectively. The shades indicate the standard deviations. All results are the 1976–2005 means. (b) The correlation between the hemispheric gradient of surface air temperature anomaly (NH-SH dTAS) and the hemispheric gradient of tropical precipitation change (NH-SH dPR). All are based on anomalies from the last 100 year means of the corresponding preindustrial control simulations. The star marks the result derived using anomalies of the reanalysis data in reference to the 1946–1975 means. The shaded area is bounded by the minimum and maximum values of all the G1 and G2 model results in HistoricalNAT. (c) Correlations between the gradient of polar to midlatitude surface temperature anomalies (Polar-Midlat Gradient of dTAS) and the mean precipitation change in the high latitudes (Highlat Mean dPR) for the Northern Hemisphere. The star marks the result derived using the anomalies of the reanalysis data in reference to the 1946–1975 means. The shaded area bounded by the minimum and maximum values of all the G1 and G2 model results in HistoricalNAT. (d) The same as Figure 3c but for the Southern Hemisphere.

3. Summary and Discussions

The results of this study have suggested that despite the fact that greenhouse gases might have been the major factor behind the global total precipitation change in the past, the distributions of such a change, however, appears to be dominated by the forcing of anthropogenic aerosols over the tropics and also substantially influenced in the extratropical regions of the Northern Hemisphere. Such a dominance of anthropogenic aerosols can be better captured by models that include prognostic aerosol and cloud microphysics features (i.e., G1 models), whereas the result of other models (i.e., G2 models) primarily reflects the effect of greenhouse gases rather than aerosols. In addition, the sharp contrast between G1 and G2 models in reproducing the observed warming in the midlatitudes and high latitudes of the Northern Hemisphere in reference to the tropics [*Ekman*, 2014] (see Table S1) and the past transient climate variations of precipitation indicates the importance of including prognostic and physically based cloud and aerosol schemes in the models. Previous studies that used the models without such schemes had thus likely an underestimated aerosol forcing similar to that of G2 models. As a result, these studies might have suggested a precipitation change pattern more or less resembling the effect of greenhouse gases (e.g., as in HistoricalGHG), especially with the peak of precipitation enhancement across the equator rather than being well confined within the southern hemispheric tropics [*Zhang et al.*, 2007; *Hwang et al.*, 2013].

Many of the precipitation changes analyzed and shown in this study occur in places away from the aerosol-laden regions, thus reflecting an effect via first the response of large-scale atmospheric dynamics to aerosol forcing, i.e., the "remote impact" of aerosols [*Wang*, 2013] rather than a local microphysical modification that needs to occur in places where aerosols present [*Tao et al.*, 2012]. Nevertheless, in certain aerosol-laden regions such as the Indian summer monsoon region, recent analyses using CMIP5 model results have also suggested the critical role of aerosols in determining the precipitation trend and pattern [*Polson et al.*, 2014; *Salzmann et al.*, 2014; *Guo et al.*, 2015].

Despite being able to produce the correct spatial distribution of precipitation change, even group 1 models used in this study still underestimate the quantity of these changes particularly in the tropics compared to the reanalysis data. This discrepancy becomes more evident if the modeled anomalies were derived using the same reference base as in analyzing the reanalysis data, i.e., the 1946–1975 mean instead of the last 100 year mean of the preindustrial control simulation. A possible reason is that currently, even the state-of-the-science models only included aerosol-cloud microphysical connection in stratiform clouds. Such a connection in deep convective clouds, a critical process particularly in the tropics [*Wang*, 2005; *Tao et al.*, 2012; *Altaratz et al.*, 2014], is still not being represented in these models. Furthermore, modeled large-scale variabilities such as ENSO still differ from observations in amplitude, period, and teleconnection [*Flato et al.*, 2013; *Salzmann and Cherian*, 2015] and thus could introduce an artificial amplification or suppression on an overlapped aerosol effect.

References

Allen, M. R., and W. J. Ingram (2002), Constraints on future changes in climate and the hydrological cycle, *Nature*, *419*, 224–232.

Altaratz, O., I. Koren, L. A. Remer, and E. Hirsch (2014), Review: Cloud invigoration by aerosols—Coupling between microphysics and dynamics, *Atmos. Res.*, *140–141*, 38–60.

Bischoff, T., and T. Schneider (2014), Energetic constraints on the position of the Intertropical Convergence Zone, *J. Clim.*, *27*, 4937–4951.

Broccoli, A. J., K. A. Dahl, and R. J. Stouffer (2006), Response of the ITCZ to northern hemisphere cooling, *Geophys. Res. Lett.*, *33*, L01702, doi:10.1029/2005GL024546.

Chiang, J. C. H., and C. M. Bitz (2005), Influence of high latitude ice cover on the marine Intertropical Convergence Zone, *Clim. Dyn.*, *25*, 477–496.

Chiang, J. C. H., and A. R. Friedman (2012), Extratropical cooling, interhemispheric thermal gradients, and tropical climate change, *Annu. Rev. Earth Planet. Sci.*, *40*, 383–412.

Compo, G. P., et al. (2011), The Twentieth Century Reanalysis Project, *Q. J. R. Meteorol. Soc.*, *137*, 1–28.

Ekman, A. M. L. (2014), Do sophisticated parameterizations of aerosol-cloud interactions in CMIP5 models improve the representation of recent observed temperature trends?, *J. Geophys. Res. Atmos.*, *119*, 817–832, doi:10.1002/2013JD020511.

Flato, G., et al. (2013), Evaluation of climate models, in *Climate Change 2013: The Physical Science Basis. Contribution of Working Group I to the Fifth Assessment Report of the Intergovernmental Panel on Climate Change*, edited by T. F. Stocker et al., Cambridge Univ. Press, Cambridge, U. K., and New York.

Forster, P. M., T. Andrews, P. Good, J. M. Gregory, L. S. Jackson, and M. Zelinka (2013), Evaluating adjusted forcing and model spread for historical and future scenarios in the CMIP5 generation of climate models, *J. Geophys. Res. Atmos.*, *118*, 1139–1150, doi:10.1002/jgrd.50174.

Guo, L., A. G. Turner, and E. J. Highwood (2015), Impacts of 20th century aerosol emissions on the South Asian monsoon in the CMIP5 models, *Atmos. Chem. Phys.*, *15*, 6367–6378, doi:10.5194/acp-15-6367-2015.

Held, I. M., and B. J. Soden (2006), Robust responses of the hydrological cycle to global warming, *J. Clim.*, *19*, 5686–5699.

Hwang, Y.-T., D. M. W. Frierson, and S. M. Kang (2013), Anthropogenic sulfate aerosol and the southward shift of tropical precipitation in the late 20th century, *Geophys. Res. Lett.*, 40, 2845–2850, doi:10.1002/grl.50502.

Kang, S. M., I. M. Held, D. M. W. Frierson, and M. Zhao (2008), The response of the ITCZ to extratropical thermal forcing: Idealized slab-ocean experiments with a GCM, *J. Clim.*, 21, 3521–3532, doi:10.1175/2007JCLI2146.1.

Lohmann, U., L. Rotstayn, T. Storelvmo, A. Jones, S. Menon, J. Quaas, A. M. L. Ekman, D. Koch, and R. Ruedy (2010), Total aerosol effect: Radiative forcing or radiative flux perturbation?, *Atmos. Chem. Phys.*, 10, 3235–3246.

Mitchell, J. F., C. A. Wilson, and W. M. Cunnington (1987), On CO_2 climate sensitivity and model dependence of results, *Q. J. R. Meteorol. Soc.*, 113, 293–322.

Myhre, G., et al. (2013), Anthropogenic and natural radiative forcing, in *Climate Change 2013: The Physical Science Basis. Contribution of Working Group I to the Fifth Assessment Report of the Intergovernmental Panel on Climate Change*, edited by T. F. Stocker et al., Cambridge Univ. Press, Cambridge, U. K., and New York.

Osborne, J. M., and F. H. Lambert (2014), The missing aerosol response in twentieth-century mid-latitude precipitation observations, *Nat. Clim. Change*, 4, 374–378, doi:10.1038/NCLIMATE2173.

Polson, D., M. Bollasina, G. C. Hegerl, and L. J. Wilcox (2014), Decreased monsoon precipitation in the Northern Hemisphere due to anthropogenic aerosols, *Geophys. Res. Lett.*, 41, 6023–6029, doi:10.1002/2014GL060811.

Ramaswamy, V., and C.-T. Chen (1997), Linear additivity of climate response for combined albedo and greenhouse perturbations, *Geophys. Res. Lett.*, 24, 567–570, doi:10.1029/97GL00248.

Rotstayn, L. D., and U. Lohmann (2002), Tropical rainfall trends and the indirect aerosol effect, *J. Clim.*, 15, 2103–2116.

Salzmann, M., and R. Cherian (2015), On the enhancement of the Indian summer monsoon drying by Pacific multidecadal variability during the latter half of the twentieth century, *J. Geophys. Res. Atmos.*, 120, 9103–9118, doi:10.1002/2015JD023313.

Salzmann, M., H. Weser, and R. Cherian (2014), Robust response of Asian summer monsoon to anthropogenic aerosols in CMIP5 models, *J. Geophys. Res. Atmos.*, 119, 11,321–11,337, doi:10.1002/2014JD021783.

Schneider, T., T. Biscoff, and G. H. Haug (2014), Migrations and dynamics of the Intertropical Convergence Zone, *Nature*, 513, 45–53, doi:10.1038/nature13636.

Shindell, D. T. (2014), Inhomogeneous forcing and transient climate sensitivity, *Nat. Clim. Change*, 4, 274–277, doi:10.1038/nclimate2136.

Tao, W.-K., J.-P. Chen, Z.-Q. Li, C. Wang, and C.-D. Zhang (2012), The impact of aerosol on convective cloud and precipitation, *Rev. Geophys.*, 50, RG2001, doi:10.1029/2011RG000369.

Taylor, K. E., R. J. Stouffer, and G. A. Meehl (2012), An overview of CMIP5 and the experiment design, *Bull. Am. Meteorol. Soc.*, 93, 485–498.

Wang, C. (2004), A modeling study on the climate impacts of black carbon aerosols, *J. Geophys. Res.*, 109, D03106, doi:10.1029/2003JD004084.

Wang, C. (2005), A modeling study on the response of tropical deep convection to the increase of CCN concentration: 1. Dynamics and microphysics, *J. Geophys. Res.*, 110, D21211, doi:10.1029/2004JD005720.

Wang, C. (2007), Impact of direct radiative forcing of black carbon aerosols on tropical convective precipitation, *Geophys. Res. Lett.*, 34, L05709, doi:10.1029/2006GL028416.

Wang, C. (2013), Impact of anthropogenic absorbing aerosols on clouds and precipitation: A review of recent progresses, *Atmos. Res.*, 122, 237–249.

Wilcox, L. J., E. J. Highwood, and N. J. Dunstone (2013), The influence of anthropogenic aerosol on multi-decadal variations of historical global climate, *Environ. Res. Lett.*, 8, 024033.

Wu, P., N. Christidis, and P. Stott (2013), Anthropogenic impact on Earth's hydrological cycle, *Nat. Clim. Change*, 3, 807–810, doi:10.1038/NCLIMATE1932.

Zhang, X., F. W. Zwiers, G. C. Hegerl, F. H. Lambert, N. P. Gillett, S. Solomon, P. A. Stott, and T. Nozawa (2007), Detection of human influence on twentieth-century precipitation trends, *Nature*, 448, 461–466.